**Constraining High-Density ERP source analysis using Functional MRI.**

Michael Worden
Department of Psychology, University of Pittsburgh, 522 LRDC
Pittsburgh, PA 15260 USA
mworden@neurocog.lrdc.pitt.edu

and

Diana J. Vincent
Department of Radiology, MUSC, 171 Ashley Ave.
Charleston, SC 29425
vincendj@musc.edu

Walter Schneider
Department of Psychology, University of Pittsburgh, 522 LRDC
Pittsburgh, PA 15260 USA
schneider+@pitt.edu

Judith M. Shedden
Department of Psychology, McMaster University,1280 Main Street West
Hamilton, Ontario L8S 4K1 Canada
shedden@coffee.mcmaster.ca

**ABSTRACT**

Mapping the global neural activity of the human brain is an extremely difficult problem. In this study using a visual cognitive task, we obtained electrophysiological data from high density Evoked Response Potentials (ERPs), which give millisecond temporal data. However, using just ERPs alone for source localization is an ill-posed problem since there are an infinite number of source configurations for any surface potential map. Magnetic Resonance Imaging (MRI) and functional MRI (fMRI) provide millimeter spatial localization of neural activity, and thus allows us to constrain the problem and avoid making assumptions. We discuss each modality, their advantages and disadvantages, how they are coregistered, and then our initial results.

*Keywords:* fMRI, ERP, colocalization, source localization, coregistration, inverse problem



Worden, M., Vincent, D. J., Schneider, W., & Shedden, J. M. (1995). Constraining High-Density ERP source analysis using Functional MRI. In M. Witten & D. J. Vincent (Eds.), Series in mathematical biology and medicine (Vol. 5, pp. 723-744). Singapore: World Scientific.

## Introduction

When we consider the relationship between cognitive and perceptual events and brain function, we want to know where in the brain these events take place. We also want to know the time course for these events, both in relationship to each other and in relation to the stimuli which initiated them (for a current commentary, see Wood, [17]). Recent advances in functional neuroimaging promise to help us ask and answer these types of questions in increasing detail. However no single imaging modality currently offers *both* high spatial resolution and high temporal resolution in the range of the time domain of cognitive processes. Our approach, along with those of several other groups of researchers (e.g., George [4]; Simpson [15]), is to use multiple imaging modalities - in our case, fMRI and high density ERPs, combined with biophysical models. We do this so that the strengths of one modality will constrain the shortcomings of the other (see Fig [1]).

## Overview of ERPs

ERPs are electrical potentials related to the cortical processing of stimuli, and recorded at the scalp. Because of the columnar organization of the cortex, small currents traveling along the apical dendrites of pyramidal cell neurons summate and produce electrical fields which may be recorded even through the electrically insulating skull (Regan [10]; Nunez [8]). It is important to note that the data which are recorded at the scalp do not correspond to any single area of cortical activity but, due to volume conduction in the skull, represent the sum of all generators active at that time.

The raw electrical data recorded from the scalp are very noisy, making it difficult to distinguish signal from the background noise. Therefore, the data corresponding to many stimulus presentations, time-locked to the presentation of the stimulus, must be averaged. In this way, the noise is averaged out leaving the signal from the processing of the stimulus. Although ERP recording provides very good temporal resolution, the spatial resolution is limited.

The general problem of identifying the cortical generators from the distribution of field potentials on the scalp is known as the inverse problem. The inverse problem in electroencephalography is mathematically ill-posed; there are an infinite number of source configurations which could generate any topography of field potentials measured at the scalp.

Conversely, the problem of determining the distribution of scalp



potentials, given a *known* set of generators, is called the forward problem. In contrast to the inverse problem, the forward problem is well characterized. There are a number of possible models one might use for solving the forward problem. The generators may be characterized as point current sources (dipoles), dipole layers, or more complex current distributions (Nunez [8]; Scherg [12]). Similarly, the models that one might use for the head range from a single homogenous sphere to complex finite-element models; the latter accurately represent the geometry of the head from which the data are collected.

The choice of a model depends on 1) the accuracy of anatomical information available, 2) the amount of computational resources available, and 3) the assumptions one is willing to make about the biophysical properties of the head and its contents. For example, structural MRI provides excellent anatomical information with high spatial resolution, making a finite element model attractive. On the other hand, with finite element models it is necessary to assign a value to the relative conductive properties of each node or element in the model. This information is not particularly well understood. Simple spherical models provide relatively simple computations for determining the surface distributions for any given set of generators, but in some cases, some error will be introduced by representing the head as a sphere.

The inverse problem becomes solvable when one has *a priori* information about the generators of the scalp voltages. In the unconstrained problem, there are six degrees of freedom for each dipole and the number of generators is not known. When one has information about the number, location and orientation of the dipoles, the problem reduces to a single degree of freedom for each generator, namely the magnitude of the dipole. Functional MRI has the potential to be useful as a source of such information.

## Overview of fMRI

Magnetic Resonance Imaging or MRI has been used for the last decade and a half to produce high quality structural anatomical images with millimeter resolution. Functional MRI is a technique which has been developed in recent years using MR imaging to measure changes in local blood-flow related to neural activity. Functional MRI exploits the paramagnetic differences between deoxygenated and oxygenated hemoglobin. Deoxygenated hemoglobin has paramagnetic properties which distort the local magnetic field. This causes an increase in signal dephasing in the surrounding tissue (T2*) and thus produces a decrease in the MR signal from that tissue. (Ogawa [9]). Neural activity increases local levels of oxygenated vs. deoxygenated hemoglobin, so active tissue has higher MR return signal relative to inactive areas. Comparing the baseline condition to the experimental one allows us to identify and quantify those regions in which the blood flow changes.

There is a lag of 3 to 6 seconds between the onset of neural activity and the peak of the local blood-flow response. The variability of this lag is one of the major factors limiting the temporal resolution of fMRI. The time course for cognitive operations, by comparison, ranges from a few to a few hundred milliseconds.

Raw fMRI images must go through a number of post-processing steps. We use a minimum size criterion for areas of activation and combine it with a split-half t-test. This rejects particles that do not show significance in both halves of the data set. This methodology is described in more detail in a recent paper by Schneider, Noll & Cohen [14]. We also use MR Angiography to reject areas of activation which are related to venous artifacts and not localized in cortical tissue.

**Experimental Paradigm**

We collected data using the same experimental paradigm in both imaging modalities (ERP and fMRI). The paradigm was a number sequence task (See figure [2]). This is a visual target detection task. In it, the subject searches for an out-of-sequence digit in a sequential series of numbers presented eccentric to a fixation point.

There were two experiments in which the locations of the stimuli were changed (Fig[3]). In one experiment the sequential stimuli appeared in the upper-left visual quadrant, in the other they appeared in the lower-right. Stimuli subtended approximately 1.5 degrees of visual angle and they were presented approximately three degree latera and three degrees above or below the horizontal meridian. So as to determine task-related areas of increased blood-flow, in the fMRI version of the experiment we added a control condition in which the subject viewed a fixation point and responded to an occasional very brief blink of that point.

We chose these two experimental conditions to elicit two differen spatial configurations of cortical activity, each having similar numbers of locations and each having about the same amount of active cortex. At least for early visual areas, different parts of the visual field project to different areas of cortex, and there are corresponding areas in the



right and the left hemispheres. Thus, each experimental condition should produce a unique (but possibly overlapping) set of active cortical areas and a correspondingly unique spatio-temporal pattern of voltages at the scalp reflecting that activity.

**Data Collection and Description**

*fMRI*

Functional MRI data were collected for a total of ten oblique coronal slices oriented so that the entire occipital lobe would be scanned. Slices were 5 mm thick with additional scan parameters as in Schneider, Casey and Noll [13]. We predicted that the different experimental conditions would produce different patterns of cortical activity. This prediction was validated by the data.

Our subject showed eleven discrete areas of activation for each condition. This number was not an *a priori* constraint; the data set itself strictly it. In both experimental conditions, most of the areas of activation were contralateral to the stimulus, only a small number of areas in more anterior occipital cortex showing both ipsi- and contralateral activation. Furthermore, the upper-field stimulation produced more ventral activation while lower-field stimuli declared more dorsally. Primate literature and human lesion data of the visula cortex predict this pattern of activation . Figure [4] illustrates an example of activation in a single slice for the two experimental conditions.

*ERP*

ERP data were collected using a 62-channel electrode montage. The montage was based on the standard 10-20 system with additional electrodes located at intermediate points between posterior electrodes, and using the right mastoid as the reference point. Data were recomputed to a reference-free representation using a distance-weighted average method (Hjorth [6]). Scalp voltages were recorded with SA Instruments amplifiers at a rate 256 Hz with 0.1-100 Hz bandpass and a time constant of 1.6 seconds. Additionally, two extra-occular electrodes identified eye movements and blinks. Trials containing such artifacts were rejected off-line and not included in the averaging process. Since the two experimental conditions produce different distributions of activity on the cortex in fMRI, we expected to see this in differential distributions of voltage patterns on the surface of the scalp, and that is what we found.

*Coregistration of the data.*

To combine data from different modalities, the two data sets must have a common frame of reference. We use a system based on three skull landmarks - the nasion and the two periauricular points (see Williamson [16]; Fig [5]). These skull landmarks and the locations of the electrodes on the scalp are recorded with a three-dimensional sonic digitizer at the time of the ERP recording session. The same landmarks can be identified on high-resolution volume scans taken during the MR sessions. An affine transformation changes the native coordinate system for one modality into the coordinate system of the other.

## Head Model

For our initial efforts, we chose to use a three-shell spherical head model where the three shells correspond to the brain, the skull, and the scalp respectively (e.g., Ary, Kline and Fender [1]). Conductivity and thickness parameters were taken from Rush and Driscoll [11]. Since our forward calculations are done using a spherical model, it is necessary to map the scalp data to the surface of the sphere. We used a least-squares procedure to solve for a best-fitting sphere to the digitized electrode points (Lutkenhoner, Pantev & Hoke [[7]). Each electrode location moves radially to the closest point on the surface of the sphere and its location represented as a pair of spherical coordinates (fig [6]).

The locations of the generators, as identified in the fMRI scans, must also be represented on the same sphere. Every location on the surface of the scalp has a corresponding pair of spherical coordinates which are determined by the best-fitting sphere. Likewise, points inside the head corresponding to the locations of cortical activity can be represented by a pair of spherical coordinates plus a third spherical coordinate which indicates the radial distance of the point from the center of the best-fit sphere. The location of each generator is then adjusted along a radius from the center of the best-fitting sphere through the generator by a value proportional to the difference between the distance to the surface of the head and the distance to the surface of the best-fitting sphere along that same radius.

The location of each generator is determined by the radially-adjusted location of the center of mass for each particle in the fMRI data. The orientation of the generators is determined by the local cortical geometry. Splines fit to the cortical ribbon along the areas of activation in orthogonal planes. A vector normal to each spline is taken at the center of mass for the particle and these vectors are combined to yield a single orientation which approximates an equivalent dipole source configuration for each area of activation.



Once we have 1) the location and orientation of each putative generator and 2) the locations of the recording sites on the surface of that sphere, we can use linear superposition to determine a matrix, **E**. **E** relates the activity at each generator to the activity at each recording site. The equation can be expressed in matrix form as

$$\mathbf{v} = \mathbf{E}\mathbf{s}, \qquad (1)$$

where v is the vector of scalp potentials at the recording sites, **E** is the matrix which describes the linear relationship between the activity at each generator and each recording site, and **s** is a vector of strengths for each dipole generator. When **v** is known, as in the case of empirical recordings, we can calculate a pseudoinverse for **E** to get an approximate solution for **s**. This solution provides the distribution of activations over all generator locations in the spherical model, which solution would most closely recreate the recorded voltage distribution which was mapped to the sphere. The voltage distributions are, of course, provided by the ERP sessions and the magnitude of activation over all of the dipoles is solved at each time point in the relevant portion of the ERP epoch. We then plot the magnitude for any given generator at successive time points and get an estimate of the time course of activation for that area of cortex.

## Results

*Example Data*

Figure 7 shows an example of data from the top-left stimulus condition. It illustrates the temporal waveforms estimated for two areas of activation represented in two different slices of the fMRI data. These wave shapes have a characteristic biphasic form common to many stimulated areas; it is is often seen in other source estimation techniques. Wave amplitudes represent the amount of activation estimated for each area at a point in time. **Note:** negative values merely represent a polarity shift, not a "negative activation," or inhibition. This technique estimates population-level activity and cannot distinguish inhibitory from excitatory processes. The x-axis shows 4 millisecond units and represents a total epoch of about 330 milliseconds. While it is too early in the analysis to make strong claims about the validity of these data, it is interesting to note the similarity in the morphology of these two waveforms and the fact that they seem to be shifted in time relative to one another. This is precisely the type of information which we hope this technique will allow us to gather.

*Validation*

Each experimental condition and corresponding configuration of generators yields a different **E** matrix describing the relationship of the generators to the scalp voltages (surface of the sphere). We made an initial assessment of relative robustness by making a comparison. We looked at the difference between 1) solutions obtained when we modeled the ERP data from one condition (e.g., left upper stimulus) with the fMRI-generator locations (**E** matrix) from the other experimental condition (right lower stim) against 2) solutions when both data sets came from the same experimental condition. When both data sets came from the same experimental condition, we could account for 80% of the variance; when different conditions were used, only 60% could be explained. See Figure [8] for an illustration.

Put another way, it was not possible to find a combination of magnitudes for the generators in one condition which would substantially reproduce the ERP data from the other. We expect that improved cortical modeling techniques will increase the size of this effect, mainly by increasing our ability to account for variance in the congruent conditions.

## Future Directions

We are now pursuing several directions for further development and refinement of this technique. These are both paradigmatic and implementational. We recognize that the paradigm which we have been using--the number sequence paradigm (see above)--is too cognitively oriented for the initial development and assessment of this technique. This task requires skilled performance by the subject both in terms of numerical processing and attentional management, i.e., the allocation of covert attentional resources. Furthermore, the strategies reported by subjects performing this task inevitably involve subvocalization of the numeric sequence. While it is precisely these kinds of issues which we ultimately want to explore and understand with these neuroimaging techniques, for initial validation it is desirable that the paradigms be kept as simple as possible. There are several reasons for this: First, we need to minimize the number of active generators likely to be involved during the task. This both simplifies the analysis and makes results more interpretable. It is especially important to do this



since a large number of brain areas are likely to be used for even simple tasks (c.f., Felleman and Van Essen [3], for a discussion of the number of different "visual" brain areas in the macaque brain). This is also why we restricted our analysis to the early part of the temporal recording epoch: we expect that later in the epoch, as a stimulus is processed, more generators become involved.

Another reason to switch to tasks which are less cognitively loaded is to allow comparisons with the existing animal literature. In the process of validating this methodology, we would like to compare our results to known findings based on intracranial, intracellular, and other invasive recording techniques which have been performed on non-human primates. This is important because much of our understanding of the human brain is derived from these models. Animal models also provide a data base for which no comparable source exists for humans. For example, in a task such as the number sequence paradigm, there are no animal data with which we may compare our results. When our results show similarities to the animal data, this lends support to the validity of our technique. Discrepancies may lead us to identify problems with our methodology or, conversely, to identify previously unknown facts about ways in which human cortical processing differs from these other species.

With regard to methodological improvements, there are several areas under development. Of primary importance is more accurate characterization of the cortical surface and the ability to relate cortical geometry to the model generators. At best this would be a fully automatic process. Several groups of researchers have developed techniques for effectively generating tessellated surfaces from high-resolution MR data (e.g., Dale and Sereno [2]; George [4]), and we will be assessing these for ease of incorporation into our computational framework. It will be important to explore the relevant parameters which may be varied in these models, for example the degree of tessellation, to determine how these affect the interpretation of the results.

For instance, we might place a generator on any tile on the reconstructed cortical surface which falls within a voxel exceeding some criterion for activation. This would tend to give clusters of individual dipoles, each with slightly different orientation and location for each discrete region of cortical activation. As an alternative, we might start with a cluster of dipoles, as described above, and then mathematically "average" them to create a single equivalent dipole for each area. We expect the time course information for computations between areas to be better served by the latter technique, whereas within area questions may be better addressed with the former. The implementation of computer-generated cortical surfaces has the additional advantage of reducing the error potentially associated with tediously fitting spline functions to the surface by hand, as we have been doing.

Further refinement of our shell-based model is expected to increase the validity of our estimates. Currently we use a model in which there are shells corresponding to the brain, skull and scalp, and the thickness parameters are predetermined. Retaining the computational advantages of an explicit shell-based model, we may increase the fidelity of the model by using a four- or a five-shell model in which an additional shell is added for the CSF and possibly the dura. Thickness parameters may be estimated directly for each subject from a high-resolution 3D structural scan taken from each subject at the time of functional scanning. Another possibility is a model in which the head is described not as concentric shells, but as many local spheres. Greenblatt [5] has found, in simulations using cadaver skulls, that the many-local-spheres method may produce results superior to those from the concentric spherical models.

## Conclusion

Because of inherent biological and mathematical limitations, no single non-invasive neuroimaging modality currently provides both spatial and temporal information about cortical activity with the high resolution necessary for the study of cognitive processes. With the advent of new imaging modalities and increase in computational power, it is becoming possible to combine different modalities so as to have the strengths of one method compensate for the weaknesses of the other.

We describe our first stages to create an environment for combining high spatial resolution fMRI data with high temporal resolution ERP data so that an estimation might be made for the time courses of the cortical generators of the ERP data. Using a visual target detection task, we collected data in both modalities and coregistered them into the same three dimensional space. The structural MRI along with the functional yielded the locations and orientations of the areas responding to the stimuli. This information was then used to estimate the distributiuon of activity over all generator locations. In this way, we approximated the location and time course for the areas of neural activation.

While these methods are still under-constrained, we believe that such techniques represent a significant advance over other methods of



cortical source localization. In the future, these techniqus will not only be applicable to cognitive studies, but may also be useful in clinical settings. Reliable characterization of the location of specific brain activity will almost certainly alter surgical approaches as well as aid in neuropsychological assessment.

## Figures

Figure 1. The top panel illustrates the type of information obtained with fMRI. Areas in red represent locations of differential blood flow indexing local neural activity. The middle panel shows the type of informtion which is recorded using ERPs. The waveforms represent the electrical potentials recorded at the scalp as a function of time. The bottom panel illustrates the goal of this project which is to provide high-resolution temporal information of the type obtained in ERP recording for the areas of activation which are seen in fMRI.

Figure 2. Illustration of the number sequence paradigm. Sequential digits appear at a location on the screen and the subject is required to respond when a digit is detected which breaks the sequence.

Figure 3. The two experimental conditions used.

Figure 4. Example of activation seen in one slice for both experimental conditions. Note that the distribution of activation is different for each condition.

Figure 5. The PPN coordinate system.

Figure 6. Fitting a sphere to the electrode locations. The red dots represent the original electrode locations as digitized at the time of recording. The blue dots show the corresponding locations for each electrode moved to the surface of the best-fitting sphere.

Figure 7. Example of time course data calculated for two areas of activation for the top-left stimulus condition.

Figure 8. Comparison of the amount of variance accounted for when the corresponding ERP and fMRI conditions are used together versus when the fMRI and ERP data are taken from different experimental conditions.



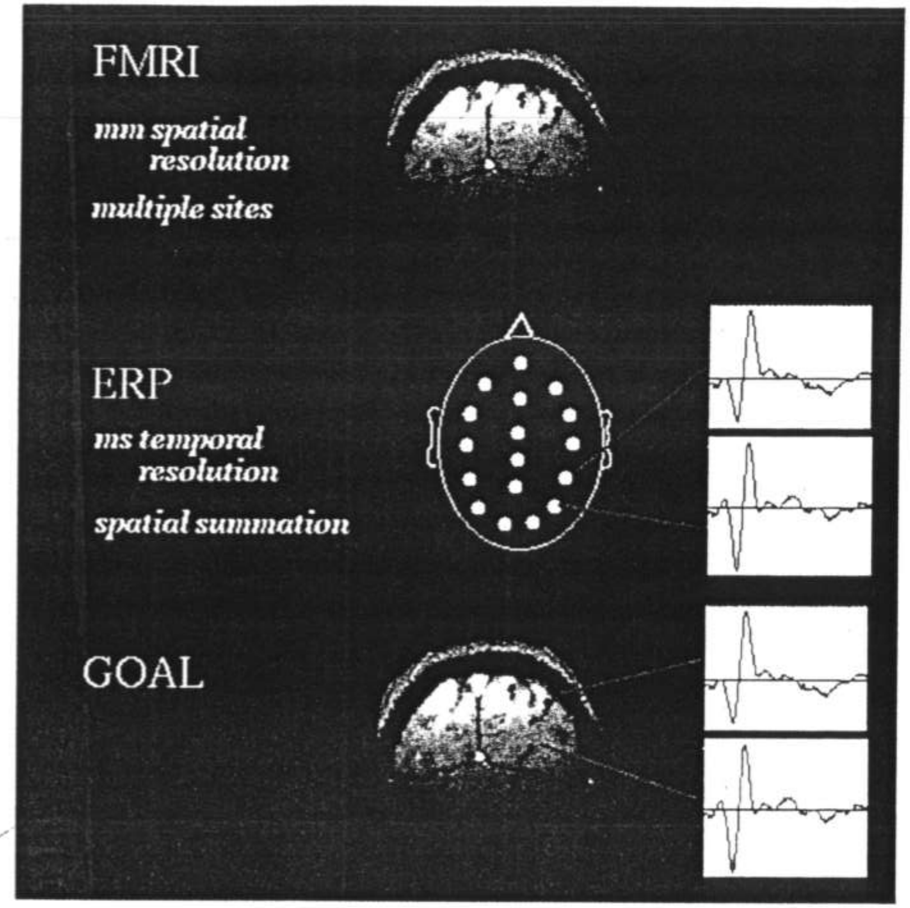


Figure 1

## Stimuli for Number Sequence Task

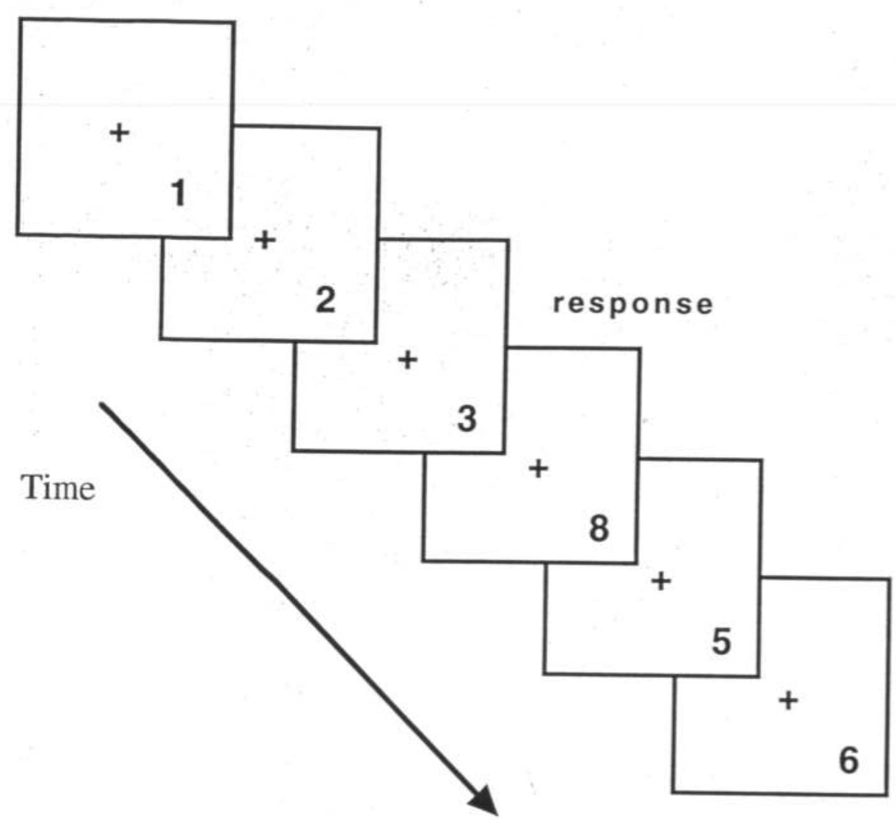


Figure 2

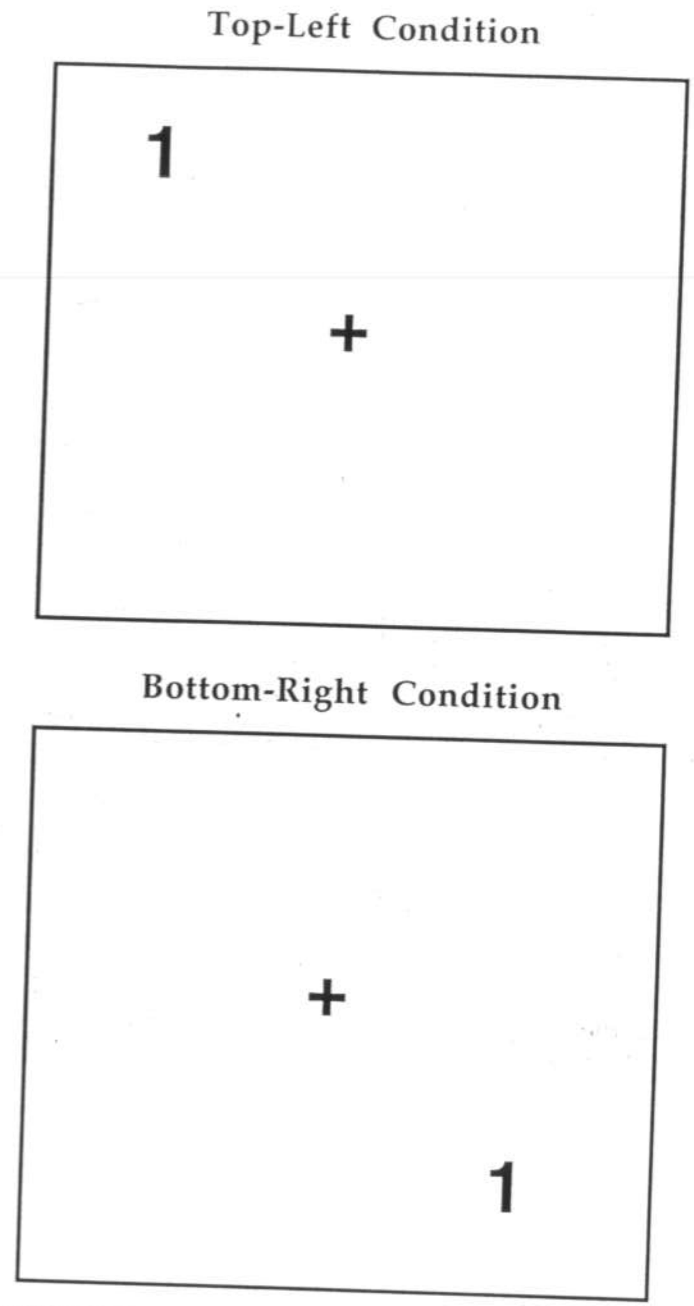


Figure 3

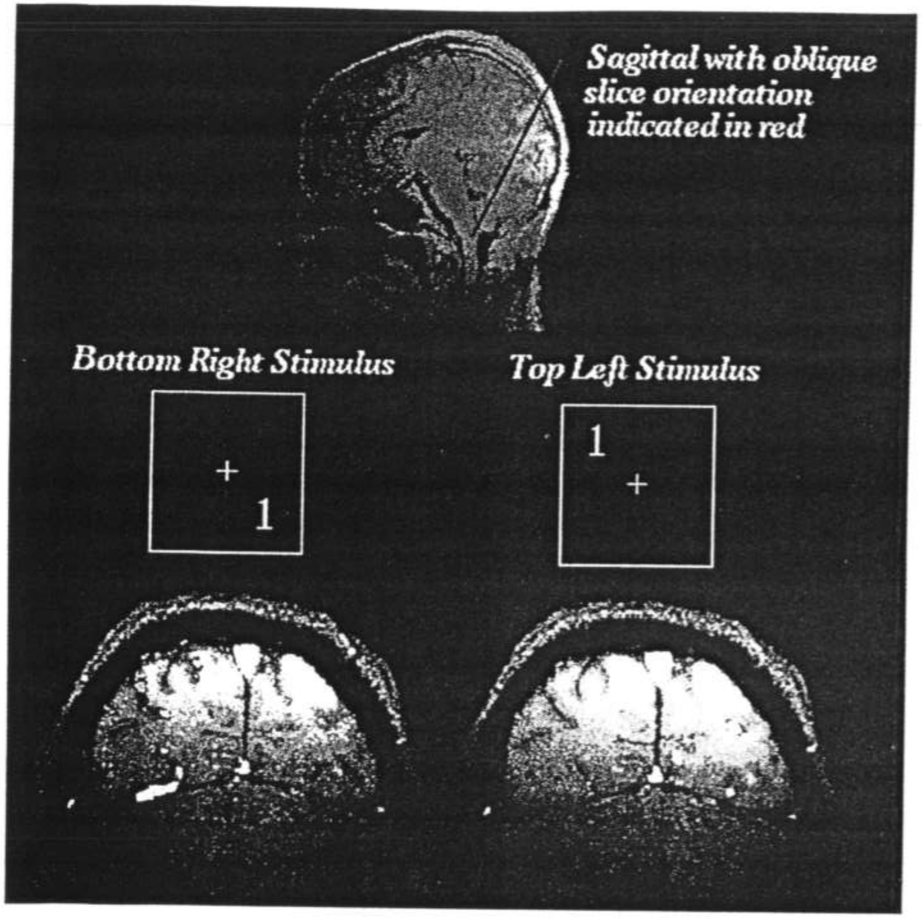


Figure 4

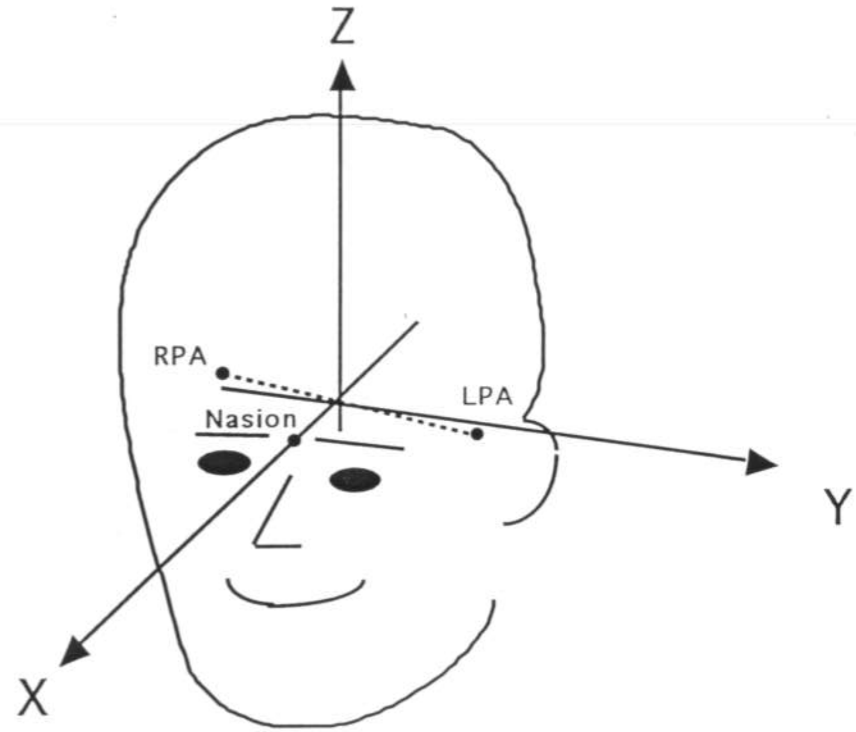


The "PPN" Coordinate System

Figure 5

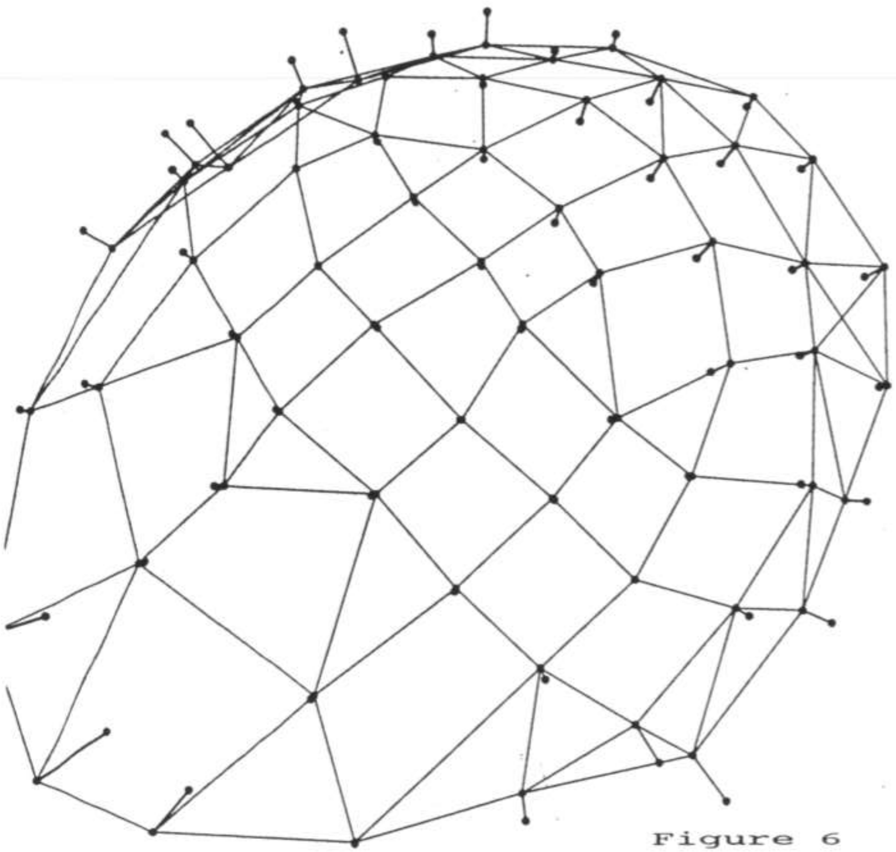

Figure 6

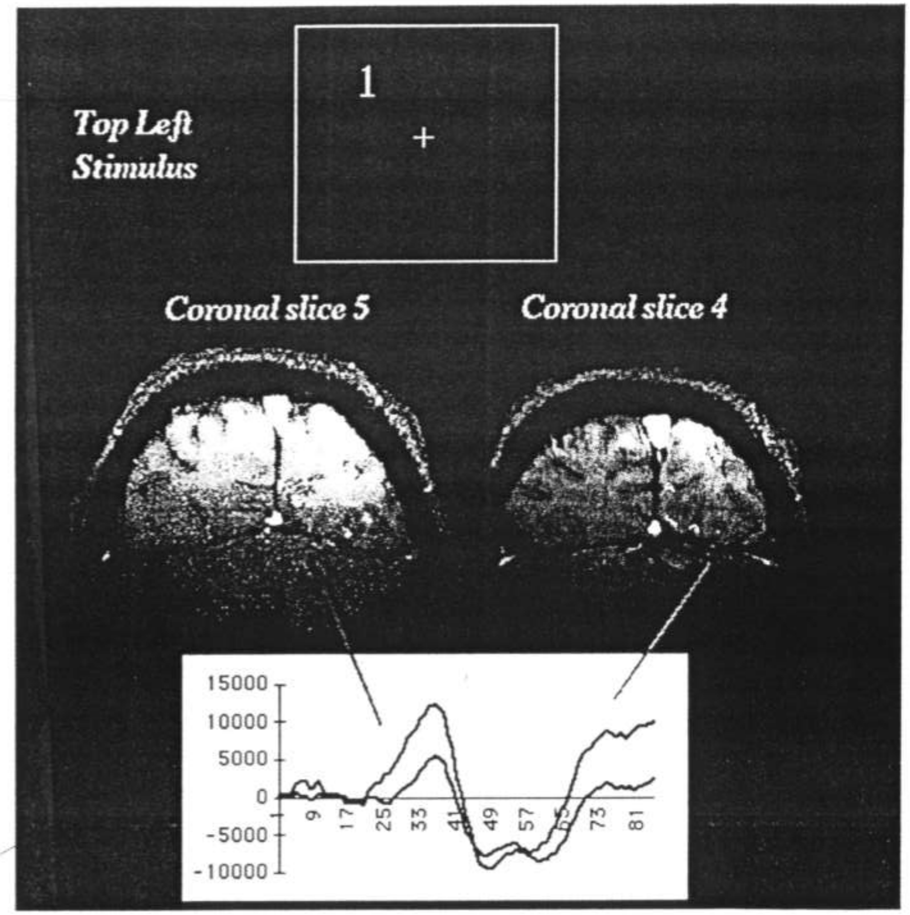


Figure 7

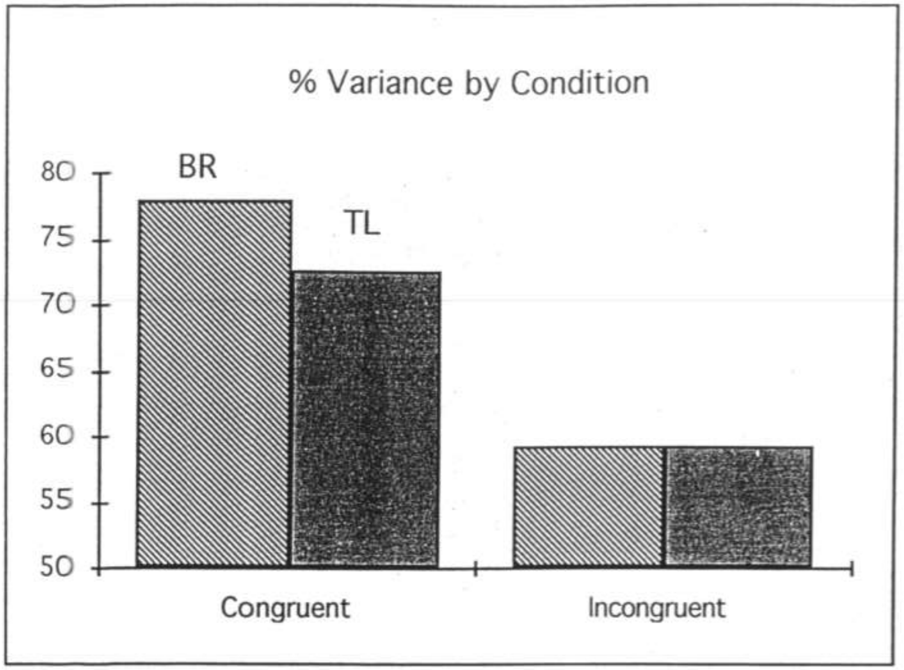


**Figure 8**

Percentage of variance accounted for when generators derived from the same experimental condition are used to model the electrical data (congruent) vs. when generators from the opposite experimental condition are used (incongruent).



### References

1. J.P. Ary, S.A. Klein, and D.H. Fender (1981). Localization of sources of evoked scalp potentials: corrections for skull and scalp thicknesses. IEEE Trans. Biomed. Eng., BME-28, 447-452.

2. A.M. Dale, and M.I. Sereno (1993). Improved localization of cortical activity by combining EEG and MEG with MRI cortical surface reconstruction: al linear approach. Journal of Cognitive Neuroscience, 5(2), 162-176.

3. D.J. Felleman and D.C. Van Essen (1991). Distributed hierarchicalprocessing in the primate cerebral cortex. Cerebral Cortex, 1(1),1-47.

4. J.S. George, C.J. Aine, J.C. Mosher, H.A. Schlitt, C.C. Wood, J.D. Lewine,and J.A. Sanders, (1994). Studies of human visioncombining MEG and anatomical and functional MRI. In Poster presented at Society for Neuroscience, 24th annual meeting, Miami Beach, Florida.

5. R.E. Greenblatt (1994). Merging multiple data supports for enhanced encephalographic source estimations. Presentation given at Workshop on Multimodal Registration, University of Chicago,Chicago.

6. B. Hjorth (1982). An adaptive EEG derivation technique. EEG and Clinical Neurophysiology, 54, 654-661.( 1).

7. B. Lutkenhoner, C. Pantev, and M. Hoke (1990). Comparison between different methods to approximate an area of the human head by a sphere. In F. Grandori, M. Hoke, & G. L. Romani (Eds.), Auditory Evoked Magnetic Fields and Electric Potentials. Advances inAudiology. (pp. 103-118). Basal, Karger.

8. P.L. Nunez (1981). Electric fields of the brain: The neurophysics of EEG. NY: Oxford University Press.

9. S. Ogawa, T.M. Lee, A.R. Kay, and D.W. Tank (1990). Brain magnetic resonance imaging with contrast dependent on blood oxygenation. Proc Natl Acad Sci USA, 87, 9868-9872.

10. D. Regan (1989). Human Brain Electrophysiology: Evoked Potentials and Evoked Magnetic Fields in Science and Medicine. New York: Elsevier.

11. S. Rush and D.A. Driscoll (1968). Current distribution in the brainfrom surface electrodes. Anaesthesia Analgesia current Res., 47,717-723.

12. M. Scherg (1989). Fundamentals of Dipole Source Potential Analysis. In M. Hoke, F. Grandori, & G. L. Romani (Eds.), Auditory Evoked Magnetic Fields and Potentials. Adv. Audiol.

13. W. Schneider, B.J. Casey, and D. Noll (1994). Functional MRI mapping of stimulus rate effects across visual processing stages. Human Brain Mapping, 1(2), 117-133.

14. W. Schneider, D.C. Noll, and J.D. Cohen (1993). Functional topographic mapping of the cortical ribbon in human vision with conventional MRI scanners. Nature, 365, 150-153.

15. G.V. Simpson, J.J. Foxe, H.G.J. Vaughan, A.D. Mehta, and C.E. Schroeder (1994). Integration of electrophysiological source analyses, MRI and animal models in the study of visual processing and attention. Journal of Electroencephalography and Clinical Neurophysiology. In press.

16. S.J. Williamson, Z. Lu, D.Karron and L. Kaufman (1991). Advantages and Limitations of Magnetic Source Imaging.

17. C.C. Wood (1994). Human brain mapping in both time and space. Human Brain Mapping, 1(4), iii-vi.